Carbohydrate Polymers 98 (2013) 276–281

Contents lists available at SciVerse ScienceDirect

Carbohydrate Polymers

journal homepage: www.elsevier.com/locate/carbpol

# Hydroxypropyl methylcellulose substituent analysis and rheological properties

Hannah Akinosho[d], Samantha Hawkins[b], Louise Wicker[a,c,*]

[a] Department of Food Science and Technology, The University of Georgia, 100 Cedar Street, Athens 30602, United States
[b] Richard B. Russell Agricultural Research Center, Agricultural Research Service, United States Department of Agriculture, 950 College Station Road, Athens, GA 30605, United States
[c] Department of Home Economics Education, College of Education, Korea University, Anam-Dong, Seongbuk-Gu, Seoul 136-701, Korea
[d] Department of Chemistry and Biochemistry, Georgia Institute of Technology, 901, Atlantic Dr., Atlanta, GA 30332, United States

ARTICLE INFO

*Article history:*
Received 20 July 2012
Received in revised form 24 May 2013
Accepted 28 May 2013
Available online 6 June 2013

*Keywords:*
Hydroxypropyl methylcellulose
FT-IR
Raman
Rheology
Crystallinity
Methylation

ABSTRACT

The methyl and hydroxypropyl substituents in hydroxypropyl methylcellulose (HPMC) affect the resulting gel properties. These substituents in five HPMC gels were characterized using Fourier transform infrared spectroscopy (FT-IR), Raman spectroscopy, small-amplitude oscillatory shear measurements, and differential scanning calorimetry (DSC). In FT-IR spectra, the most intense peak appeared at 1053 $cm^{-1}$, denoting the presence of the glucose ring. The ratio of peak intensities at 1452 $cm^{-1}$, which represents —C—H absorptions, and at 1053 $cm^{-1}$ ($I_{1452}/I_{1053}$) and percent methylation from gas chromatography exhibited a linear association ($r^2 = 0.6296$). The broadening of the Raman spectra indicated that the relative crystallinity of HPMC decreases with increasing hydroxypropyl contents. DSC showed no linear relationship between the percent hydroxypropylation in HPMC and the percentage of free water in an HPMC gel. Small-amplitude oscillatory shear measurements revealed that the formation of an entanglements networks and/or weak gel depends on substituent contents.



## 1. Introduction

Native cellulose is linked by β-(1→4) glucosidic linkages; hydrogen bonding between neighboring cellulose chains provides mechanical strength in plants and renders cellulose insoluble in water. In caustic solution, the hydrogen bonds between cellulose chains are disrupted, and cellulose swells and absorbs water. In the swollen state, hydroxyl groups are randomly substituted with alkyl substituents such as ethyl, methyl or hydroxypropyl groups to produce a modified cellulose. The relative hydrophobicity or hydrophilicity of the substituent groups affects the solution properties of modified cellulose (Heiko Thielking & Schmidt, 2000). In hydroxypropyl methylcellulose, cellulose contains methyl and hydroxypropyl substituents that are etherified onto the cellulose backbone (Heiko Thielking & Schmidt, 2000). The position, nature, and proportion of substituents affect the resulting properties of HPMC. The substituents have been widely analyzed to assess the changes in the functionality of HPMC. The degree of substitution on HPMC and temperature influences the intermolecular interactions such as the onset of turbidity during heating, termed cloud point (Greiderer, Steeneken, Aalbers, Vivó-Truyols, & Schoenmakers, 2011; Mitchell et al., 1993), the onset of gelation (Haque, Richardson, Morris, Gidley, & Caswell, 1993; Sarkar, 1995), drug release rates (Viridén, Wittgren, Andersson, & Larsson, 2009), and the viscoelastic properties of the gel (Bodvik et al., 2010).

Cloud point describes the phase separation of HPMC dispersions at sufficiently high temperatures, which is manifested as a cloudy solution. The relationship between substituent content and cloud point has been studied through the enzymatic degradation of HPMC. Highly substituted regions of HPMC experienced less enzymatic degradation than less substituted regions. These fragments, which differed by substitution, were used in cloud point studies; fragments with higher proportions of substituted regions produced the largest shifts in cloud points at the transmission at 50%, $T_{50}$, when using UV–vis (Schagerlöf et al., 2006). The heterogeneity of distribution of the substituents in HPMC, possessing the same substituent contents and viscosities, has also been analyzed with respect to release rates of pharmaceuticals. The findings demonstrated that slower drug release rates were associated with more heterogeneous substitution patterns (Viridén et al., 2009).

The extent and nature of substitution influence the viscoelastic properties and affect the application of HPMC in the pharmaceutical, chemical, and food industries. The hydroxypropyl and methyl contents affect the gelling abilities of HPMC. Larger quantities of

* Corresponding author at: Department of Food Science and Technology, The University of Georgia, 100 Cedar Street, Athens 30602, United States.
Tel.: +1 706 542 1055; fax: +1 706 542 1050.
*E-mail address:* lwicker@uga.edu (L. Wicker).

0144-8617/$ – see front matter © 2013 Elsevier Ltd. All rights reserved.
http://dx.doi.org/10.1016/j.carbpol.2013.05.081

hydroxypropyl substituents result in weaker gels and lower temperatures for the onset of gelation (Haque et al., 1993). The gels formed can provide an extended release matrix for pharmaceuticals (Viridén, Larsson, & Wittgren, 2010) or be used to enhance the rheological properties of foods such as surimi (Chen, 2007). Establishing structure function relationships based on the substituent content, position, and distribution provide insight into the final characteristics of the gel (Viridén, Larsson, Schagerlöf, & Wittgren, 2010). Limited research characterizes HPMC and its gels based on the methyl to hydroxypropyl ratio and substituent content. Understanding the role of substituents in gel formation is useful in the optimization and selection of HPMC for industrial uses. This study uses attenuated total reflectance Fourier transform infrared spectroscopy (ATR/FT-IR), Raman spectroscopy, differential scanning calorimetry (DSC), and small-amplitude oscillatory shear measurements to characterize the gelling and structural behavior of HPMC as related to its methyl and hydroxypropyl substituents.

## 2. Materials and methods

The five grades of HPMC were supplied by Samsung Fine Chemicals (Seoul, Korea) and differed by the percent methylation, percent hydroxypropylation, and viscosity (Pa S). The data regarding percent hydroxypropylation and percent methylation were supplied by the manufacturer and acquired using gas chromatography (Table 1).

### 2.1. Dispersion preparation

HPMC dispersions were prepared by adding 2 g of powdered HPMC into 100 mL of Type II water at 80 °C. The dispersions were stirred during addition and cooling, until the final temperature reached 25 °C. The dispersions were hydrated for 10 d at 4 °C prior to testing (Šklubalová & Zatloukal, 2008).

### 2.2. Attenuated total reflectance/Fourier transform infrared spectroscopy

The ATR–FT-IR spectra of the five grades of HPMC were obtained using a purged Nicolet 6700 FT-IR Spectrometer (Thermo Electron, Madison, WI) with a diamond crystal ATR (attenuated total reflectance) accessory (Durascope, Smiths Detection, Danbury, CT) and a DTGS detector. A background reading was taken prior to each series of measurements. Spectra of the powdered samples were collected at 25 °C using 64 scans and at a resolution of 4 $cm^{-1}$ and were background subtracted. The spectral region ranged from 4000 $cm^{-1}$ to 500 $cm^{-1}$.

### 2.3. Raman spectroscopy

Powdered HPMC were analyzed by Sentinel Sure-Cal Spectroscopy (Bruker Optics, Ettlingen, Germany). Samples weighing 4 g were placed in 5 mL glass scintillation vials and capped. The calibration of the instrument was performed automatically prior to each reading. The readings, which consisted of one scan, were taken at a power of 300 mW with a spectral region of 2250 $cm^{-1}$ to 250 $cm^{-1}$. Contributions made from the glass vials were subtracted from each spectrum prior to analysis.

### 2.4. Differential scanning calorimetry

Aliquots of 10–15 mg of 2% (w/w) HPMC were weighed into aluminum pans with pins (Cat. No.: ME-00027331, Mettler Toledo, Columbus, OH). The aluminum DSC pans were hermetically sealed and handled with forceps during testing. The samples were heated from −50 °C to 30 °C at a rate of 10 °C/min. The peaks were analyzed and integrated using the STARe 9.10 software (Mettler Toledo, Columbus, OH). The baselines were calculated using an integrated horizontal baseline, and the peaks were normalized to the weights of the samples. The enthalpy change associated with the energy associated with the melting of loosely bound water in the HPMC solutions ($\Delta H_{fusion}$) was recorded. The differential scanning calorimeter DSC 1 (Mettler Toledo, Columbus, OH) was calibrated using 6–8 mg of indium standard in an aluminum pan with a pin. An empty aluminum pan with a pin served as the reference pan during calibration and testing. The standard was heated at a rate of 10 °C/min through a range of 100–200 °C. The DSC data were collected to associate the amount of free water in the solution of HPMC with the respective HPMC grade. The percentage of free water in each solution was calculated using Eq. (1) (Anghel & Saitō, 2003).

$$\text{Percentage of free water} = \frac{\Delta H_{fusion}(\text{free water in HPMC solution})}{\Delta H_{fusion}(\text{pure water})} \times 100 \quad (1)$$

### 2.5. Dynamic oscillatory measurements

Dynamic oscillatory measurements were conducted on the stress-controlled SR-5000 rheometer (Rheometric Scientific, TA Instruments, New Castle, DE). The gap was set to 0.50 mm, and the cone angle was 4°. A strain sweep was conducted at a frequency of 1 Hz on each of the hydrated samples to determine linear viscoelastic region (LVR). The lowest strain in the viscoelastic region for each HPMC was determined and used in the frequency sweeps of the five samples. A 0.3% strain was used for AN6 and AN50 between frequencies of 0.05 Hz and 5 Hz while 1% strain was used for BN40M, CN40H, and CN10T. A strain of 1.0% could not be used in the analysis of AN6 and AN50 because the linear viscoelastic regions differed between samples and did not coincide during the dynamic strain sweep. The elastic modulus ($G'$), loss modulus ($G''$), and tan $\delta$ were collected using a cone (35 mm) and Peltier plate at 25 °C (±0.01 °C).

### 2.6. Statistical analysis

All measurements were conducted on triplicate dispersions. Statistical analyses were performed using the Minitab® 15 software. Significant differences between means were assessed using one-way ANOVA and the $t$-test at $P < 0.05$.

## 3. Results and discussion

### 3.1. ATR–FT-IR

The peaks obtained from the FT-IR spectrum were used to (1) analyze the structure of HPMC and (2) correlate peak ratios with the percent methylation provided by the manufacturer as determined by gas chromatography. In the FT-IR spectra of the HPMC (Fig. 1), many of the observed bands appeared in the fingerprint region, which encompasses wavenumbers between 1400 and 900 $cm^{-1}$. The five HPMC produced similar spectra but differed in intensity of certain peaks. The most intense peak in the spectra occurred at 1053 $cm^{-1}$, represents out-of-phase vibrations associated with an alkyl substituted cyclic ring containing ether linkages. The peak at 944 $cm^{-1}$ represents the in-phase vibrations from ether linkages and appears as a weaker band attached to the band at 1053 $cm^{-1}$ (Coates, 2006). Cellulose material possesses glucose molecules that contain one ether linkage in the ring structure and another ether linkage between neighboring glucose molecules (Teegarden, 2004). The spectra obtained reflecting the ether bonds (1053 and 944 $cm^{-1}$) verify the presence of these ethers in the structure of

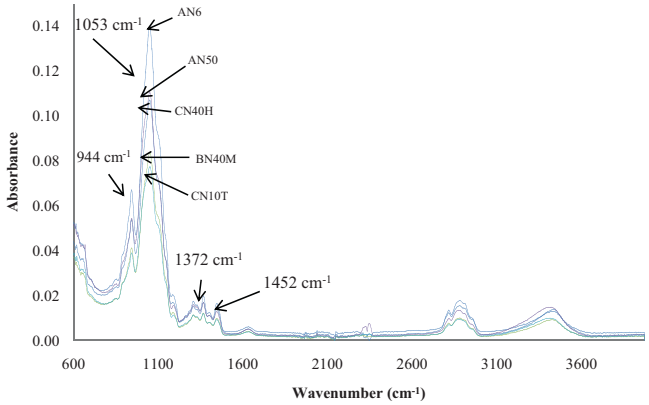


**Fig. 1.** The FT-IR spectra of the five HPMC.

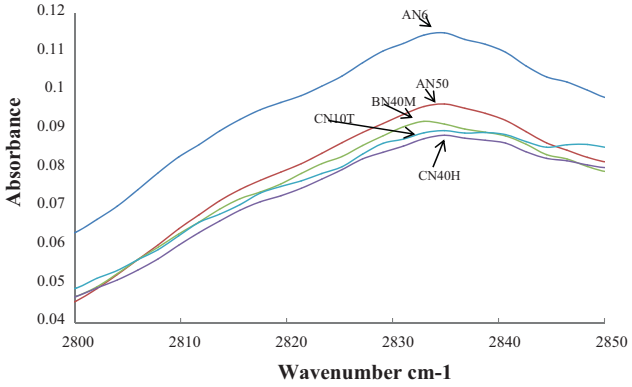


**Fig. 2.** The normalized FT-IR spectra of the five HPMC between 2850 and 2800 $cm^{-1}$ to demonstrate difference in the methyl content. The different intensities of the peaks at 2835 $cm^{-1}$ provide indications of the methyl contents of the HPMC.

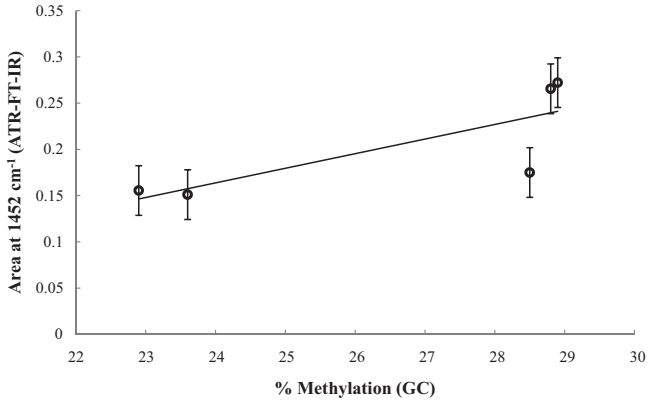


**Fig. 3.** The figure above depicts the association between the percent methylation from gas chromatography and the area under the curve as represented by ATR–FT-IR. Samsung Fine Chemicals analyzed the substituent content using gas chromatography.

glucose as well as ether linkages involved in covalent bonding of the substituents.

Hydroxyl groups on the hydroxypropyl substituents and glucose rings at carbon two and three represent secondary alcohols; the C—O bonds involved in the secondary alcohol structure typically exhibit absorption at 1100 $cm^{-1}$ (Coates, 2006). Between 1091 and 1130 $cm^{-1}$, a shoulder appears on the most intense band in the spectrum. The midpoint of the shoulder occurs at 1112 $cm^{-1}$ and may indicate the C—O bonds in secondary alcohols. Finally, the band arising from O—H bonds from the primary alcohol at C6 on the glucose molecule appears at 1312 $cm^{-1}$ (Coates, 2006; Langkilde & Svantesson, 1995). The bands representing primary and secondary alcohols reveal that unsubstituted carbons remain on the glucose rings in the cellulose backbone after etherification.

The peaks at 1372 and 1452 $cm^{-1}$ resulted from C—H bending and stretching modes from methyl groups; these peaks are very weak relative to others in the spectrum (Coates, 2006). Wang, Dong, and Xu (2007) analyzed the structure of HPMC using FT-IR and identified the peaks at 1458 and 1378 $cm^{-1}$ as methyl C—H vibrations. The peaks at 2835 and 2898 $cm^{-1}$ represent the absorptions of C—H vibration modes from methyl groups. The normalized peak intensities at 2835 $cm^{-1}$ against the largest peak in the spectra (1053 $cm^{-1}$) indicate that the $I_{2835}/I_{1053}$ is associated well with the methyl contents. The pattern of normalized peak intensities follows the order of percent methylation from least to greatest as determined by gas chromatography (GC): CN40H < CN10T < BN40M < AN50 < AN6 (Table 1 and Fig. 2). While the trend between absorbance followed the declared percent methylation, the $r^2$ was 0.4141.

To form an association between the degree of methylation as determined by ATR/FT-IR and GC, the peak at 1452 $cm^{-1}$ was used as it unambiguously represents C—H bonds in HPMC. The area under the curve at 1452 $cm^{-1}$ was calculated using the OMNIC 7.0 software (Thermo Electron Corporation, Madison, WI) and associated with the percent methylation as determined by GC. The area determined by FT-IR was plotted against the percent methylation calculated using GC. A weak, linear association exists between the percent methylation and the area under the curve at 1452 $cm^{-1}$ between 22.0% and 30.0% methylation ($y = 0.0158x - 0.2153$; $r^2 = 0.6296$). This indicates that data provided by ATR/FT-IR spectra is a sufficient predictor of the methyl content of HPMC (Fig. 3). Although the differences in percent methylation are small, FT-IR discriminates between the methyl contents well. These results support the peak intensities observed in the normalized FT-IR spectrum. Similar studies have been performed using FT-IR that successfully established the degree of esterification or methylation in pectins using peak intensities (Chatjigakis et al., 1998; Manrique & Lajolo, 2002; Synytsya, Čopıĭková, Matějka, & Machovič, 2003). For example, these methods used peaks that represented carboxylic acid groups to estimate the degree of methylation of pectin. Inferences regarding the degree of hydrox-

**Table 1**
Physicochemical characteristics[a] and percent free water, peak onset (°C), and temperature of onset (°C) of HPMC from experimental DSC[b] thermograms of five HPMC.

| HPMC | %M[a] | %HP[a] | M:HP[a] ratio | Viscosity[a] (Pa s) | Free water[b] (%) | Peak onset[b] (°C) | Onset temperature[b] (°C) |
|---|---|---|---|---|---|---|---|
| AN6 | 28.9 | 9.4 | 3.07 | 0.006 | 97.34a ± 0.007 | −2.24a ± 0.44 | −2.73a ± 1.06 |
| AN50 | 28.8 | 8.6 | 3.34 | 0.051 | 94.77b ± 0.014 | −2.12a ± 0.50 | −2.21a ± 0.44 |
| BN40M | 28.5 | 6.4 | 4.45 | 0.402 | 95.78b ± 0.009 | −2.11a ± 0.32 | −2.13a ± 0.57 |
| CN40H | 22.9 | 8.7 | 2.63 | 3.990 | 94.90b ± 0.022 | −2.35a ± 0.17 | −2.52a ± 0.93 |
| CN10T | 23.6 | 8.8 | 2.68 | 115.115 | 95.48b ± 0.0133 | −2.45a ± 0.18 | −1.94a ± 0.59 |

[a] The %M, percent methyl, %HP, percent hydroxypropyl, M:HP ratio and viscosity measurements were declared by manufacturer; viscosity measurements were made in a 2% (w/w) at 25 °C dispersion of HPMC.
[b] Different letters (a and b) reflect significant differences in means in each column ($P < 0.05$).

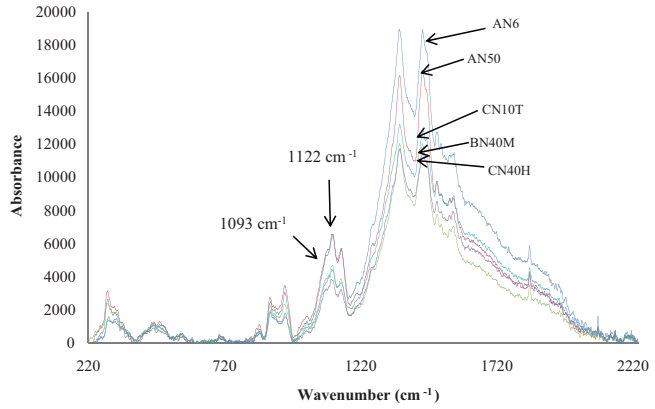


**Fig. 4.** The superimposed Raman spectra of the five grades of HPMC are pictured above. Broadening of each spectrum is apparent in the 1220–2220 $cm^{-1}$ range.

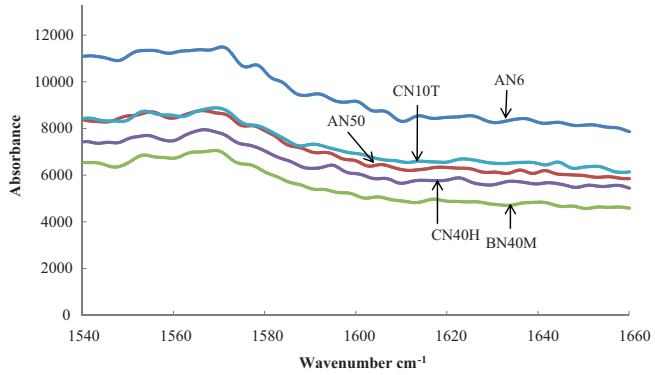


**Fig. 5.** Broadening of the Raman spectrum of each HPMC between 1540 $cm^{-1}$ and 1660 $cm^{-1}$. BN40M possesses the narrowest spectrum, while AN6 possesses the broadest spectrum.

ypropylation as predicted by FT-IR could not be established due to the failure to unambiguously assign any alcohol derived absorption to the hydroxypropyl group alone.

### 3.2. Raman spectroscopy

The Raman spectra of the HPMC samples are depicted in Fig. 4 and provide complementary spectral information to the FT-IR spectra. The maximum wavenumber for the Sentinel SureCal was 2250 $cm^{-1}$; as a result, the peaks corresponding to wavenumbers greater than 2250 $cm^{-1}$ were not displayed. The Raman spectra obtained were similar to those previously reported (Davies et al., 1990; Langkilde & Svantesson, 1995). The most intense peaks in the spectrum occurred at 1358 and 1453 $cm^{-1}$, which are C—H vibrations from methyl groups. The band at 1120 $cm^{-1}$ and the shoulder at 1093 $cm^{-1}$ correspond to a six membered ring bound by ether linkages, while the peak at 1155 $cm^{-1}$ corresponds to an alkyl substituted ether (Coates, 2006; Langkilde & Svantesson, 1995). A second peak corresponding to ether linkages was observed at 946 $cm^{-1}$ (Coates, 2006). Langkilde and Svantesson (1995) identified bands at 1097 and 1122 $cm^{-1}$ as bands arising from unsubstituted glucose. These bands verify that all glucose molecules do not participate in the etherification reaction.

In a Raman spectrum, polymers containing more amorphous regions possess broader peaks, while polymers with more crystalline regions contain narrower peaks (Agarwal, Reiner, & Ralph, 2010; Schenzel, Fischer, & Brendler, 2005). In Fig. 5, the most noticeable broadening occurs in the right shoulder of the most intense peaks in the spectrum in the region 1540–1660 $cm^{-1}$. As a result, this region was selected as an indicator of relative crystallinity. In a similar study using Raman to assess the crystallinity of hydroxyapatite, the normalized full width at half maximum (FWHM) was selected as the region of interest (Pucéat, Reynard, & Lécuyer, 2004). BN40M appears to possess the narrowest spectrum, which indicates the greatest number of crystalline regions in its structure. AN6, however, possesses the widest spectrum which is indicative of the larger number of amorphous regions in its structure as compared to the other four grades of cellulose. The differences in crystallinity of mixtures of pure crystalline and purely amorphous cellulose have been quantified using peak ratios from Raman spectroscopy; the researchers identified peaks that were most responsive to changes in crystallinity and made predictions using peak ratios that were very close to the theoretical crystallinities (Agarwal et al., 2010).

The order of increasing broadening at the midpoint of this region 1606 $cm^{-1}$ is as follows: BN40M < CN40H < AN50 < CN10T < AN6. The amount of crystalline character in a polymer affects its mechanical strength; larger proportions of crystalline regions are associated with increased mechanical strength (Young & Lovell, 1991). The order or increasing amorphous character closely resembles the pattern of increasing percentage of hydroxypropyl groups: BN40M < AN50 < CN40H < CN10T < AN6. The findings in this experiment suggest that higher contents of hydroxypropyl substituents lower the crystallinity of HPMC, which may have implications in the strengths of the gels that are formed.

When considering the viscoelastic nature of gels, the degree of crystallinity affects the deformation modulus. More specifically, the deformation modulus is directly proportional to the degree of crystallinity (Cowie, 1991). The crystallinity of a modified cellulose, such as HPMC, becomes lower after the addition bulky hydroxypropyl substituents, which prevent close packing of neighboring chains (Silva et al., 2008). Studies have demonstrated that hydroxypropyl groups in different varieties of HPMC decrease the elastic character of viscoelastic gels as well as gel strengths (Bodvik et al., 2010; Mitchell et al., 1993). The hydrophilic hydroxypropyl substituents also impede particle aggregations through entropic and steric means, leading to a weakening of gel firmness (Viridén, Larsson, et al., 2010).

### 3.3. Differential scanning calorimetry

The data obtained from DSC thermograms demonstrated that the onset of melting occurs near −2.25 °C and was not different between different HPMC samples (Table 1). The percentage of free water in the HPMC dispersions was >95%. The percentage of free water in the AN6 dispersions was significantly different from the percentage of free water in the dispersions containing AN50, BN40M, CN40H, and CN10T ($P < 0.05$). The peak temperature associated with the phase transition (peak onset) and the temperature of onset were not significantly between the different HPMC samples ($P < 0.05$). The percentage of free water in the dispersions was not linearly associated with the percentage of hydroxypropyl groups present in the sample.

In polymer solutions, water exists in three forms: bound, loosely bound, and free water. Bound water is tightly bound to the polymer and does not participate in phase transitions such as melting and evaporation. Loosely bound water undergoes the phase transitions but depresses or elevates the temperature at which the phase transition occurs. Free water experiences a phase change at the same temperature as pure water (Ford, 1999). The transitions in this experiment were attributed to the freezing point depression of loosely bound water. Because bound water does not participate in phase transitions, the enthalpy change of a solution of HPMC relative to the enthalpy change associated with pure Millipore water is linked to the loosely bound water.

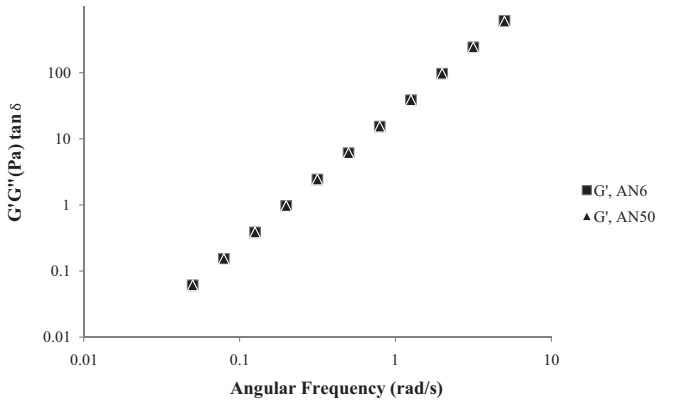


**Fig. 6.** Strain-controlled frequency sweep of AN6 and AN50 dispersions. Variation of $G'$ (filled) with angular frequency (rad/s) for AN6 and AN50 at a strain of 0.3%. $G''$ and tan $\delta$ are not shown because only $G'$ was observed during the frequency sweep.

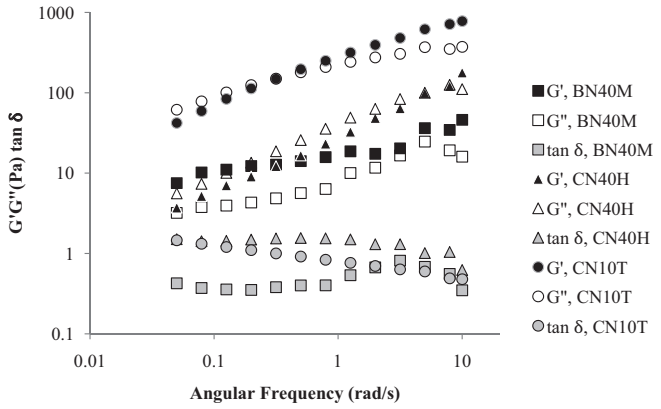


**Fig. 7.** Strain-controlled frequency sweep for BN40M, CN40H, and CN10T. Variation in $G'$ (filled), $G''$ (empty), and tan $\delta$ (gray) with angular frequency (rad/s) for BN40M, CN40H, and CN10T at a strain of 1.0%.

In polymers, increasing numbers of hydrophilic groups are associated with increasing quantities of loosely bound water (Anghel & Saitō, 2003). However, no linear relationship was observed between either the hydrophobic or hydrophilic substituents in HPMC and the free water content in hydrated HPMC (Mitchell et al., 1993). Similar results were obtained in this experiment. In addition to the hydroxypropyl content, several variables affect water binding in polymer dispersions; these variables include polymer crystallinity, substituent arrangement, crosslinking, and degree of substitution (Franks, 1988). The variation in each of these characteristics may be responsible for the discrepancy in forming a linear relationship between these variables. The peak onset during a freezing point depression depends on the concentration of solute, which may account for the lack of significant differences between HPMC types (Engel & Reid, 2006). The concentration of HPMC in the dispersion did not vary between each variety which may account for the similarity in peak onset and temperature of onset. The results suggest that DSC is unsuitable to make inferences about the amount of free water in an HPMC dispersion based on the hydroxypropyl content.

### 3.4. Rheological studies

In the plot of log angular frequency against log $G'$, log $G''$, and log tan $\delta$ for AN6 and AN50 (Fig. 6), the elastic modulus dominates and is similar for both HPMC during the frequency sweep. Through rheological measurements, gels are classified as either strong gels, weak gels, or entanglement networks (Chen & Dickinson, 1998). Below a certain critical concentration, an HPMC dispersion is characterized as a dilute solution lacking entanglements of polymer chains (Phillips & Williams, 2000). Strong gels exhibit the typical viscoelastic behavior of gels under small deformations, until a critical point is reached. Weak gels, however, do not display viscoelastic behavior past small deformations. The properties of weak gels resemble a compromise between dilute solutions and strong gels. Under small deformations, weak gels produce $G'$ values that are one to two orders of magnitude greater than $G''$. However at higher frequencies, their three dimensional structure decomposes (Lapasin & Pricl, 1999). The plots generated during the frequency sweep of AN6 and AN50 suggest that they are dilute solutions lacking entanglements. In viscoelastic systems, $G'' > G'$ at low frequencies; a crossover eventually occurs, and thereafter $G' > G''$ at high frequencies (Goddard & Gruber, 1999). In the plots of AN6 and AN50 dispersions (Fig. 6), $G'$ dominates the frequency sweep with no prior crossover. The absence of a crossover suggests that the crossover occurred at a frequency that could not be detected by the rheometer. One prominent characteristic of entanglement networks include dominance of $G'$ during the frequency sweep (Chen & Dickinson, 1998; Phillips & Williams, 2000; Yaszemski, 2003). The plots generated during the frequency sweep of BN40M, CN40H, and CN10T (Fig. 7) suggest that these dispersions display characteristics of weak gels. For example, $G'$ and $G''$ display a slight dependence on frequency and are parallel to one another during the frequency sweep. Additionally, $G'$ dominates the entire frequency sweep suggesting it also displays the characteristics of an entanglement network (Chen & Dickinson, 1998; Yaszemski, 2003). The tan $\delta$ of BN40M, CN40H, and CN10T are greater than 0.1, suggesting that they are at least partially characterized as weak gels (Mandala, Savvas, & Kostaropoulos, 2004).

The results have demonstrated that the different methyl and hydroxypropyl contents affect whether the dispersion is described as a dilute solution, an entanglement network, a weak gel, or a strong gel after gelation. The HPMC possessing the lowest M:HP ratios (CN40H and CN10T) produced gels that resembled weak gels, while the HPMC possessing the highest M:HP ratio formed the gel that possessed both the characteristics of an entanglement network and weak gel. The HPMC with the intermediate M:HP ratios produced characteristics of an entanglement network. Overall, it appears that the dispersion behavior during the frequency sweep is dependent on the methyl content. The crossover occurs earliest in CN40H then CN10T; the differences in methylation are 22.9% and 23.6%, respectively. Furthermore, BN40M displays the characteristics of a weak gel and an entanglement network.

## 4. Conclusion

The methyl and hydroxypropyl contents of HPMC affect its gelling behaviors and structural properties. Hydroxypropyl groups are a useful indicator of the crystalline nature of the HPMC according to the data gathered by Raman. Furthermore, the crystallinity patterns observed in Raman were useful in predicting the gel strengths obtained during the strain-controlled frequency sweep. Information of the crystalline content and methyl content can aide in the selection of HPMC and preparation of gels that are ideal for a particular industrial application. The distribution of the different types of water appears to be independent of the substituent content or distribution, meaning that DSC is not a suitable method of assessing the free water content of an HPMC gel. However, FT-IR can be applied to assess the degree of methylation in an unknown HPMC sample.

## References


Agarwal, U., Reiner, R., & Ralph, S. (2010). Cellulose I crystallinity determination using FT–Raman spectroscopy: Univariate and multivariate methods. *Cellulose*, *17*(4), 721–733.

Anghel, D. F., & Saitō, S. (2003). *Aqueous polymer–cosolute systems: Special issue in honor of Dr. Shuji Saito*. Springer.

Bodvik, R., Dedinaite, A., Karlson, L., Bergström, M., Bäverbäck, P., Pedersen, J. S., et al. (2010). Aggregation and network formation of aqueous methylcellulose and hydroxypropylmethylcellulose solutions. *Colloids and Surfaces A: Physicochemical and Engineering Aspects*, *354*(1–3), 162–171.

Chatjigakis, A. K., Pappas, C., Proxenia, N., Kalantzi, O., Rodis, P., & Polissiou, M. (1998). FT-IR spectroscopic determination of the degree of esterification of cell wall pectins from stored peaches and correlation to textural changes. *Carbohydrate Polymers*, *37*(4), 395–408.

Chen, H.-H. (2007). Rheological properties of HPMC enhanced Surimi analyzed by small- and large-strain tests. I. The effect of concentration and temperature on HPMC flow properties. *Food Hydrocolloids*, *21*(7), 1201–1208.

Chen, J., & Dickinson, E. (1998). Viscoelastic properties of protein-stabilized emulsions: Effect of protein–surfactant interactions. *Journal of Agricultural and Food Chemistry*, *46*(1), 91–97.

Coates, J. (2006). Interpretation of infrared spectra, a practical approach. In *Encyclopedia of analytical chemistry*. John Wiley & Sons, Ltd.

Cowie, J. M. K. G. (1991). *Polymers: Chemistry and physics of modern materials*. Nelson Thornes.

Davies, M. C., Binns, J. S., Melia, C. D., Hendra, P. J., Bourgeois, D., Church, S. P., et al. (1990). FT Raman spectroscopy of drugs in polymers. *International Journal of Pharmaceutics*, *66*(1–3), 223–232.

Engel, T., & Reid, P. J. (2006). *Physical chemistry*. Pearson Benjamin Cummings.

Ford, J. L. (1999). Thermal analysis of hydroxypropylmethylcellulose and methylcellulose: Powders, gels and matrix tablets. *International Journal of Pharmaceutics*, *179*(2), 209–228.

Franks, F. (1988). *Water science reviews 3: Water dynamics*. Cambridge University Press.

Goddard, E. D., & Gruber, J. V. (1999). *Principles of polymer science and technology in cosmetics and personal care*. Marcel Dekker.

Greiderer, A., Steeneken, L., Aalbers, T., Vivó-Truyols, G., & Schoenmakers, P. (2011). Characterization of hydroxypropylmethylcellulose (HPMC) using comprehensive two-dimensional liquid chromatography. *Journal of Chromatography A*, *1218*(34), 5787–5793.

Haque, A., Richardson, R. K., Morris, E. R., Gidley, M. J., & Caswell, D. C. (1993). Thermogelation of methylcellulose. Part II. Effect of hydroxypropyl substituents. *Carbohydrate Polymers*, *22*(3), 175–186.

Heiko Thielking, & Schmidt, M. (2000). Cellulose ethers. In *Ullmann's encyclopedia of industrial chemistry*. Wiley-VCH Verlag GmbH & Co. KGaA.

Langkilde, F. W., & Svantesson, A. (1995). Identification of celluloses with Fourier-Transform (FT) mid-infrared, FT-Raman and near-infrared spectrometry. *Journal of Pharmaceutical and Biomedical Analysis*, *13*(4/5), 409–414.

Lapasin, R., & Pricl, S. (1999). *Rheology of industrial polysaccharides: Theory and applications*. Springer.

Mandala, I. G., Savvas, T. P., & Kostaropoulos, A. E. (2004). Xanthan and locust bean gum influence on the rheology and structure of a white model-sauce. *Journal of Food Engineering*, *64*(3), 335–342.

Manrique, G. D., & Lajolo, F. M. (2002). FT-IR spectroscopy as a tool for measuring degree of methyl esterification in pectins isolated from ripening papaya fruit. *Postharvest Biology and Technology*, *25*(1), 99–107.

Mitchell, K., Ford, J. L., Armstrong, D. J., Elliott, P. N. C., Hogan, J. E., & Rostron, C. (1993). The influence of substitution type on the performance of methylcellulose and hydroxypropylmethycellulose in gels and matrices. *International Journal of Pharmaceutics*, *100*(1–3), 143–154.

Phillips, G. O., & Williams, P. A. (2000). *Handbook of hydrocolloids*. CRC Press.

Pucéat, E., Reynard, B., & Lécuyer, C. (2004). Can crystallinity be used to determine the degree of chemical alteration of biogenic apatites? *Chemical Geology*, *205*(1/2), 83–97.

Sarkar, N. (1995). Kinetics of thermal gelation of methylcellulose and hydroxypropylmethylcellulose in aqueous solutions. *Carbohydrate Polymers*, *26*(3), 195–203.

Schagerlöf, H., Johansson, M., Richardson, S., Brinkmalm, G., Wittgren, B., & Tjerneld, F. (2006). Substituent distribution and clouding behavior of hydroxypropyl methyl cellulose analyzed using enzymatic degradation. *Biomacromolecules*, *7*(12), 3474–3481.

Schenzel, K., Fischer, S., & Brendler, E. (2005). New method for determining the degree of cellulose I crystallinity by means of FT Raman spectroscopy. *Cellulose*, *12*(3), 223–231.

Silva, S. M. C., Pinto, F. V., Antunes, F. E., Miguel, M. G., Sousa, J. J. S., & Pais, A. A. C. C. (2008). Aggregation and gelation in hydroxypropylmethyl cellulose aqueous solutions. *Journal of Colloid and Interface Science*, *327*(2), 333–340.

Šklubalová, Z., & Zatloukal, Z. (2008). Optimization of regression equation for prediction of viscosity of aqueous solutions of the cellulose derivatives. *Pharmaceutical Development and Technology*, *13*(5), 359–365.

Synytsya, A., Čopıĭková, J., Matějka, P., & Machovič, V. (2003). Fourier transform Raman and infrared spectroscopy of pectins. *Carbohydrate Polymers*, *54*(1), 97–106.

Teegarden, D. M. (2004). *Polymer chemistry: Introduction to an indispensable science*. NSTA Press, National Science Teachers Association.

Viridén, A., Larsson, A., Schagerlöf, H., & Wittgren, B. (2010). Model drug release from matrix tablets composed of HPMC with different substituent heterogeneity. *International Journal of Pharmaceutics*, *401*(1/2), 60–67.

Viridén, A., Larsson, A., & Wittgren, B. (2010). The effect of substitution pattern of HPMC on polymer release from matrix tablets. *International Journal of Pharmaceutics*, *389*(1/2), 147–156.

Viridén, A., Wittgren, B., Andersson, T., & Larsson, A. (2009). The effect of chemical heterogeneity of HPMC on polymer release from matrix tablets. *European Journal of Pharmaceutical Sciences: Official Journal of the European Federation for Pharmaceutical Sciences*, *36*(4/5), 392–400.

Wang, L., Dong, W., & Xu, Y. (2007). Synthesis and characterization of hydroxypropyl methylcellulose and ethyl acrylate graft copolymers. *Carbohydrate Polymers*, *68*(4), 626–636.

Yaszemski, M. J. (2003). *Tissue engineering and novel delivery systems*. Marcel Dekker Incorporated.

Young, R. J., & Lovell, P. A. (1991). *Introduction to polymers*. Chapman and Hall.